IEEE Access
Multidisciplinary ⋮ Rapid Review ⋮ Open Access Journal

Received 23 May 2024, accepted 27 May 2024, date of publication 30 May 2024, date of current version 7 June 2024.

Digital Object Identifier 10.1109/ACCESS.2024.3407654

RESEARCH ARTICLE

The Reinartz Oscillator: Analysis Beyond Regular Behavior of the Circuit

JIRI PETRZELA, ONDREJ KALLER, AND JIRI VAVRA
Department of Electrical Engineering, University of Defence, 662 10 Brno, Czech Republic

Corresponding author: Jiri Petrzela (jiri.petrzela@unob.cz)

This work was supported in part by the Ministry of the Interior of the Czech Republic through the Instant Signal Processing Using Hybrid Systems in Defence Infrastructure under Grant VK01030060, and in part by the Institutional Support (VAROPS) of the Ministry of Defence of the Czech Republic.

ABSTRACT This paper is focused on nonlinear behavior associated with fourth-order autonomous lumped circuit known as the Reinartz oscillator. It is shown that this naturally sinusoidal oscillator with three-winding transformer can exhibit robust chaotic behavior. Essential scalar polynomial nonlinearity is not intrinsic to transformer, but to active two-port element described by impedance parameters. The existence of complex solutions is proved on numerical as well as experimental basis. In the first case, conventional routines for qualitative analysis of dynamical flows were applied, based on either prescribed set of differential equations or generated data sequence. In detail, a pair of the largest Lyapunov exponents are visualized with respect to key system parameters, attractor dimensions, recurrence plots and bifurcation diagrams showing interesting routes-to-chaos scenarios are provided to illustrate complexity of observed steady state motion. For the second case, electronic circuits dynamically equivalent to investigated mathematical model will be designed, constructed, and experimentally measured. Chaotic signals captured as oscilloscope screenshots will be compared to theoretical counterparts.

INDEX TERMS Chaos, hyperchaos, sinusoidal oscillator, Reinartz oscillator, impedance parameters, Lyapunov exponents, two-port modeling, strange attractors, recurrence plots, Lyapunov exponents.

I. INTRODUCTION

Despite relative rich history of research work done in the field of nonlinear dynamics and chaotic circuits, complex and unpredictable time evolution of electronic systems still attracts interest of many design engineers. Chaos in this sense can be roughly understood as a solution characterized by waveforms having continuous and broadband frequency spectrum which resembles noise. Although signals seem to be random, are generated by deterministic system without probability functions or uncertain entries. Chaotic systems, thanks to specific formation of vector field that guarantee stretching and folding of state trajectories, have additional unique properties such as extreme sensitivity to very small changes in initial conditions, dense and bounded attractors. Also, very frequently, chaotic and hyperchaotic dynamical systems exhibit significant sensitivity to changes of internal parameters. On the other hand, certain degree of structural stability (in the meaning of the vector field geometry) is required for practical applications of chaos. One can easily find examples of new modulation [1], [2], [3] techniques, novel encryption methods that somehow utilize chaotic dynamics [4], [5], [6], analog and digital secure communication principles [7], [8], random bit, multi-state or number generators [9], [10], and many others.

During intensive research of chaos in the last four decades, significant attention was paid to describe, model, analyze and classify complex phenomena in nonlinear electronic systems. To date, chaotic behavior in different forms has been observed in many well-known structures of analog building blocks, starting with continuous-time frequency filters that contain various active elements and ending with digital systems with logic gates. A brief list of these discoveries is summarized in [11] and categorized regarding to the original determination of the circuit. Of course, other comprehensive review papers and books can be found as well. To put this work into the context of discoveries made so far, naturally sinusoidal oscillators forced into chaotic regimes should be

The associate editor coordinating the review of this manuscript and approving it for publication was Ludovico Minati.

reviewed and discussed briefly. Let's start our short journey with paper [12] where authors study many different topologies of famous Wien-bridge sinusoidal oscillators from the perspective of chaotic dynamics and evolution of complex state attractor. The same network structure, but with fractional order memristor, is topic of contribution [13]. Phase shift oscillators also belong to RC feedback oscillators that can be easily turned into generators of chaos, as experimentally evidenced in work [14]. Probably the most favorite oscillator for radio-frequency applications is Colpitts circuit, where active element (usually bipolar transistor) is supplemented by positive feedback with single inductor and two capacitors. Robust chaotic regimes within this simple circuit structure are discussed in paper [15]. Parasitic capacitance intrinsic to common-emitter transistor stage is inevitable if high frequency model of transistor is considered. This element completes resonant tank in work [16] where author demonstrate existence of chaos in such configuration via practical experiments. Chaotic two-stage Colpitts oscillator and its overall analysis is described in paper [17]. After reciprocal change of capacitors and inductors the so-called Hartley sinusoidal oscillator can be obtained. In this case, complex behavior including chaos was pointed out in [18], but only on simulation basis. A more sophisticated study of this kind of oscillator is provided in [19]. There, JFET and tapped coil is used as core engine for chaos evolution. Substitution of series resonant circuit instead of inductor in Colpitts topology gives rise to the Clapp oscillator, basically fourth order autonomous dynamical system, where evolution of either chaos or hyper-chaos was proved in paper [20]. There, the concept of generalized transistor is introduced, i.e., active element is modeled as two-port using admittance parameters. Of course, description of general active device using impedance parameters is possible as well. Chaotic self-oscillations in circuit where impedance-oriented active two-port is completed with positive feedback that consists of dual-wind transformer is described in paper [21]. It is demonstrated that both impedance and admittance two-port models of bipolar transistor can result in a system with chaotic behavior. To end this list, papers [22], [23] present a group of chaotic electronic systems having one or two transistors, developed more-less by using heuristic approach. In the first case, inductor less single supply networks are presented, attractive from practical application viewpoint. In contrast to chaotic oscillators mentioned before, hysteresis nonlinearity is considered, leading to chaotic orbit that jump between a pair of unstable equilibria. In the latter case of paper, 49 unique and very simple circuits with chaotic solution were described. Authors state that random search was performed, followed by manual adjustment of some circuit component toward chaotic states. There, standard off-the-shelf transistors have been used, supported by realistic bias point setting.

The motivation of this work is to show that the heart of the Reinartz sinusoidal oscillator can serve as steady state chaos generator. The presence of chaos in lower order fundamental models of signal processing blocks is the promise of even more complicated motion if complete system is considered. The mathematical order of the system and, consequently, probability to observe complex behavior, is raised by adding working accumulation elements, by considering ubiquitous parasitic properties of active devices, by coupling or blocking components. Also, it is not an exceptional case if a numerical analysis of naturally non-chaotic analog functional block reveals chaotic dynamics with specific and useful properties. For example, autonomous chaotic systems having interesting formation of vector field, equilibrium structure, complexity of strange attractor, significant values of entropy, dynamical flow unpredictability or attractor density. Paper contributes to this problem, addressed structure of the Reinartz oscillator will be reduced to the simplest form. Moreover, bipolar transistor will show up to be replaceable by nonlinear resistor.

The organization of this paper is as follows. Second section deals with derivation process toward mathematical model of investigated fourth-order autonomous dynamical system, the so-called Reinartz sinusoidal oscillator. A small piece of linear analysis is given here, just as introductory part to optimization procedure able to localize chaotic motion in hyperspace of internal system parameters. Third section provides graphical outputs resulting from standard numerical algorithms applied on system with revealed ''sets of chaotic parameters''. It is demonstrated that chaos is neither numerical artifact nor long transient. Fourth section represents harbinger of experimental verification. Analog chaotic oscillator that is flow-equivalent to analyzed simplified Reinartz oscillator are designed in step-by-step manner. The robustness of discovered strange state attractors, showing its insensitivity to discretization of solved differential equations, rounding errors and similar problems that generally arise in numerical integration process, is clearly demonstrated. Finally, some concluding remarks are given.

II. MATHEMATICAL MODEL OF OSCILLATOR

Mathematical modeling plays a crucial role in qualitative and quantitative analysis of physical dynamical systems. The final model should be maximally simple, sufficiently accurate and reliable with respect to investigated phenomena. In electronic circuits that process large signals, the presence of nonlinearity should be considered. Simultaneously, for the high frequency circuit operation, additional accumulation elements should be connected to terminals of modeled active devices, respecting the inertial behavior of element. Therefore, even fundamental mathematical models of lower-order oscillators can be subject of chaotic oscillations. Parasitic accumulation elements can raise mathematical order of circuit, more degrees of freedom simultaneously increase probability of chaos or allow hyper-chaotic self-oscillations.

Suppose lumped electronic circuit illustrated in Fig. 1. This sinusoidal oscillator was initially dedicated for generation of single-tone signals in frequency band from tens of kHz up to units of MHz. The biasing point of bipolar transistor can be calculated after shorting all inductors and replacing capacitor by disconnection of branch. Having biasing point

transformed into numerical values of four impedance parameters, external passive circuit component count decreases to four, as indicated in Fig. 2. This is the right place to state that a three-winding transformer is employed, but only two coils are magnetically coupled.

Moreover, linear magnetic coupling will be assumed such that impedance matrix of three-port can be expressed as

$$\begin{pmatrix} L_1 & 0 & \pm M_1 \\ 0 & L_2 & \pm M_2 \\ \pm M_1 & \pm M_2 & L_3 \end{pmatrix} \cdot \frac{d}{dt} \begin{pmatrix} i_1 \\ i_2 \\ i_3 \end{pmatrix} = \begin{pmatrix} v_1 \\ v_2 \\ v_3 \end{pmatrix}, \quad (1)$$

where L_k is self-inductance of k-th winding, M_n is a mutual coupling between n-th and third coil. Signs associated with individual mutual coupling coefficient represent case studies: situation of cooperative (+) or competing (–) magnetic flows. In upcoming numerical analysis, $M_{1,2}$ will be fixed parameters, as these are related to a physical construction of transformer. Conventional quasi-linear analysis can answer the question about natural oscillation frequency and conditions for which circuit produce oscillations with stable amplitude. However, despite many passive circuit elements being removed, further symbolic calculation leads to enormously complicated fourth-order characteristic equation with only little understandable explanatory value. Thence, reasonable simplifications need to be adopted. By considering typical values of circuit elements, properties of transformer and parameters of bipolar transistor, oscillation mechanism is restricted to parallel resonant tank and oscillation frequency is defined by famous Thomson rule

$$f_{osc} = \frac{1}{2\pi\sqrt{L_3 C}}. \quad (2)$$

Schematic provided in Fig. 3 represents circuit structure of the Reinartz oscillator with bipolar transistor modeled as two-port by four impedance parameters: linear input and output impedance z_{11} and z_{22} respectively, linear backward trans-resistance z_{12} and scalar polynomial odd-symmetrical forward trans-resistance z_{21} of the form

$$z_{21}(i) = \alpha \cdot i^3 + \beta \cdot i. \quad (3)$$

Saturation-type nonlinearity typical for large signal models of active elements are respected by condition $\alpha < 0$ and $\beta > 0$. Straightforward analysis leads to following system of ordinary differential equations (ODE)

$$\begin{aligned} \frac{d}{dt}v_C &= -\frac{1}{C}i_1, \frac{d}{dt}i_1 = \frac{1}{L_3}\left(v_C - M_1\frac{d}{dt}i_2 - M_2\frac{d}{dt}i_3\right), \\ \frac{d}{dt}i_2 &= \frac{1}{L_1}\left[(z_{12} - z_{11} - z_{22})\, i_2 + z_{11}\cdot i_3 - z_{21}(i_3 - i_2)\right. \\ &\quad \left. -M_1\frac{d}{dt}i_1\right], \\ \frac{d}{dt}i_3 &= -\frac{1}{L_2}\left[z_{12}\cdot i_2 + z_{11}(i_3 - i_2) + M_2\frac{d}{dt}i_3\right], \end{aligned} \quad (4)$$

where state vector is composed by four items $\mathbf{x} = (v_C, i_1, i_2, i_3)^{\mathrm{T}}$. Lets introduce magnetic coupling coefficient for $j = 1, 2$

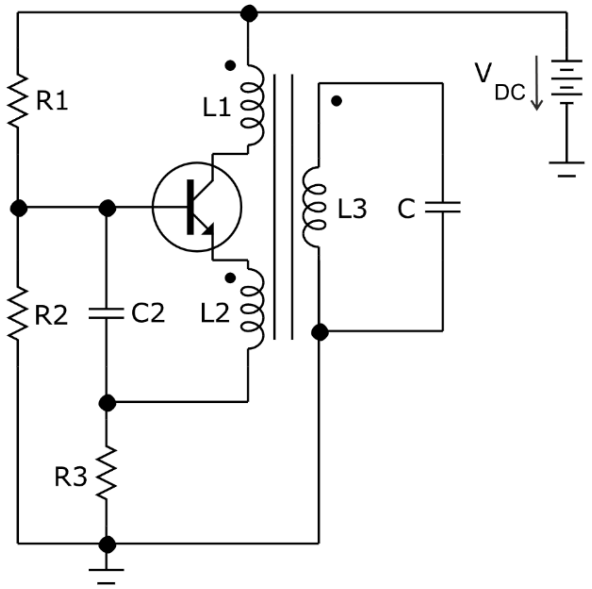

FIGURE 1. The Reinartz oscillator, full circuit configuration commonly used in practical applications.

as circuit quantity

$$k_j = M_j^2 / (L_j \cdot L_3), \quad (5)$$

and define group of three auxiliary constants

$$\begin{aligned} \Delta &= -\frac{1}{1 - k_1^2 - k_2^2}, \varepsilon = \frac{z_{11}(M_1 \cdot L_2 - M_2 \cdot L_1)}{L_1 \cdot L_2 \cdot L_3}, \\ \delta &= \frac{M_1 \cdot L_2 (z_{12} - z_{zz} - z_{22}) - M_2 \cdot L_1 (z_{12} - z_{11})}{L_1 \cdot L_2 \cdot L_3}. \end{aligned} \quad (6)$$

Note that at least one mutual coupling needs to be different from zero. Having these definitions, set of ODE (where state variables are normalized with respect to both frequency and impedance) that as ready for further numerical investigation will be

$$\begin{aligned} \frac{d}{dt}v_C &= -\frac{1}{C}i_1 \\ \frac{d}{dt}i_1 &= \frac{1}{1 - k_1^2 - k_2^2}\left[\frac{v_C}{L_3}\right. \\ &\quad - \frac{M_1 \cdot L_2 (z_{12} - z_{11} - z_{22}) - M_2 \cdot L_1 (z_{12} - z_{11})}{L_1 \cdot L_2 \cdot L_3} i_2 \\ &\quad \left. - \frac{z_{11}(M_1 \cdot L_2 - M_2 \cdot L_1)}{L_1 \cdot L_2 \cdot L_3} i_3 - \frac{M_1}{L_1 \cdot L_3} z_{21}(i_3 - i_2)\right] \\ \frac{d}{dt}i_2 &= -\frac{M_1}{L_1 \cdot L_3 (1 - k_1^2 - k_2^2)} v_C \\ &\quad + \left[\frac{z_{12} - z_{11} - z_{22}}{L_1} + \frac{M_1 \cdot \delta}{L_1 (1 - k_1^2 - k_2^2)}\right] i_2 \\ &\quad + \left[\frac{z_{11}}{L_1} + \frac{M_1 \cdot \varepsilon}{L_1 (1 - k_1^2 - k_2^2)}\right] i_3 \\ &\quad + \frac{M_1 - L_1 \cdot L_3}{L_1^2 \cdot L_3} z_{21}(i_3 - i_2) \end{aligned}$$

$$\frac{d}{dt}i_3 = -\frac{M_2}{L_2 \cdot L_3 \left(1-k_1^2-k_2^2\right)}v_C + \left[\frac{z_{11}-z_{12}}{L_2} + \frac{M_2 \cdot \delta}{L_2\left(1-k_1^2-k_2^2\right)}\right] i_2 + \left[\frac{M_2 \cdot \varepsilon}{L_2\left(1-k_1^2-k_2^2\right)} - \frac{z_{11}}{L_2}\right] i_3 + \frac{M_1 \cdot M_2}{L_1 \cdot L_2 \cdot L_3\left(1-k_1^2-k_2^2\right)} z_{21}\left(i_3 - i_2\right), \quad (7)$$

where $1-k_1^2-k_2^2 \neq 0$. Note that eleven system parameters are involved, and this number needs to be reduced. Of course, the process of mathematical model reduction must respect basic physical principles that apply in analog circuits.

Our purpose is to find as simple circuit model as possible but still exhibiting two features: initial Reinarz-like topology and robust chaotic self-oscillations (no input driving signal). Parameter space dedicated for optimization-based searching-for-chaos routine can be significantly reduced by considering hypothetical biasing point of generalized bipolar transistor. Assume negligible backward trans-resistance and active two-port operation as ideal current-controlled voltage-source, i.e., with zero input $z_{11} = 0\ \Omega$ and zero output $z_{22} = 0\ \Omega$ resistance. After that, the second coil becomes shorted, and the order of mathematical model decreases to three. Numerical analysis of this situation with beginnings of coil windings as indicated in Fig. 2 does not show chaotic attractors. However, if collector coil is wounded in reverse fashion, numerical results become more promising. Now we are speaking about circuit provided in Fig. 4 and described by following set of ODE

$$\frac{d}{dt}v_C = -\frac{1}{C}i_A$$
$$\frac{d}{dt}i_A = \frac{1}{L_3}\left[v_C + M_1\frac{d}{dt}i_C\right]$$
$$\frac{d}{dt}i_C = \frac{1}{L_1}\left[-M_1\frac{d}{dt}i_A + z_{21}\left(i_C\right)\right], \quad (8)$$

which can be rewritten in form more convenient for numerical analysis as

$$\frac{d}{dt}v_C = -\frac{1}{C}i_A$$
$$\frac{d}{dt}i_A = \frac{1}{L_3}\left[\left(1-\frac{M_1^2}{L_1 \cdot L_3 + M_1^2}\right)v_C + \frac{M_1}{L_1 \cdot L_3 + M_1^2} z_{21}\left(i_C\right)\right]$$
$$\frac{d}{dt}i_C = -\frac{M_1}{L_1 \cdot L_3 + M_1^2}v_C + \frac{L_3}{L_1 \cdot L_3 + M_1^2} z_{21}\left(i_C\right), \quad (9)$$

where the new state vector is $\mathbf{x} = (v_C, i_A, i_C)^{\mathrm{T}}$. Obviously, only mutual coupling between first and third coil remains active. Note that the investigated circuit de-facto represents nonlinear resistor with cubic polynomial ampere-voltage characteristics inductively coupled with simple resonant tank.

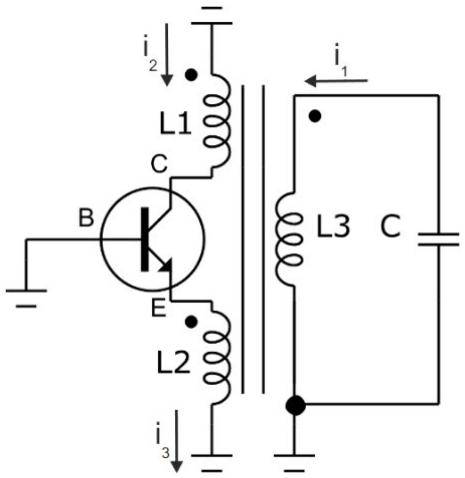

FIGURE 2. The Reinartz oscillator, simplified fourth-order network ready for linear AC analysis.

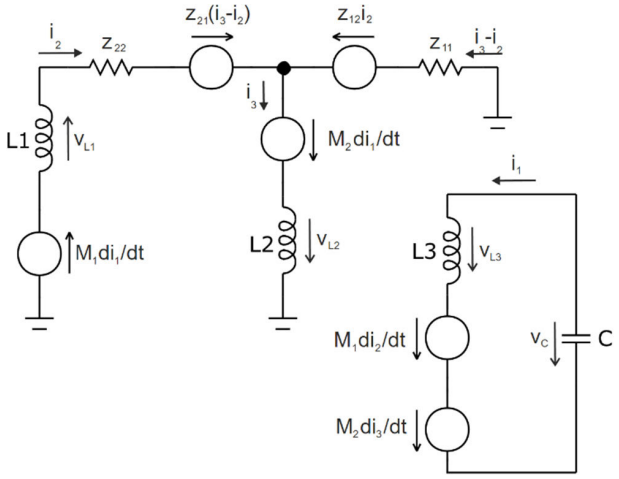

FIGURE 3. The Reinartz oscillator, schematic with bipolar transistor modeled as two-port by four impedance parameters.

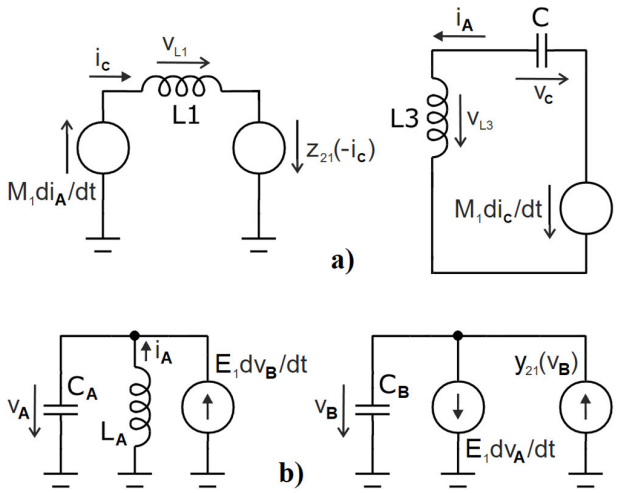

FIGURE 4. The Reinartz oscillator without mutual coupling between second and third coil leading to third-order system: a) circuit structure with single current-controlled voltage-source, b) dual oscillator.

This represents significant difference if compared to ''mature study'' of fourth order autonomous system presented in paper [24].

For experimental verification, a chaotic system containing two inductors can be transformed into dual equivalent with single inductor. Corresponding circuitry is provided in Fig. 4, where E_1 represents, in fact, static coupling of two capacitors. Mathematical model consists of formally the same set of ODE as system (7), but with circuit quantities and passive elements interchanged by their duals, namely

$$\begin{aligned}\frac{d}{dt}i_A &= -\frac{1}{L_A}v_A\\ \frac{d}{dt}v_A &= \frac{1}{C_A}\left[i_A + E_1\frac{d}{dt}v_B\right]\\ \frac{d}{dt}v_B &= \frac{1}{C_B}\left[-E_1\frac{d}{dt}v_A + y_{21}\,(v_B)\right].\end{aligned} \tag{10}$$

III. NUMERICAL ANALYSIS OF REDUCED MODEL

Regarding numerical values of internal parameters, origin of state space is always equilibrium point of analyzed dynamical system (9). Considering time derivatives equal zero in system (8) one can easily learn that there are additional equilibrium points placed symmetrically with respect to origin, namely in positions

$$\boldsymbol{x}_{eq} = \left(v_C^{eq} \quad i_A^{eq} \quad i_C^{eq}\right)^T = \left(0\ 0\ \pm\sqrt{-\tfrac{\beta}{\alpha}}\right)^T, \tag{11}$$

Optimization routine used to reveal dynamical motion with specific fingerprints deals with self-excited attractors, namely those excited directly by fixed point located at origin of state space. Thus, state space origin is kept unstable, and this rule represents first step toward calculation of objective function. To preserve this feature, at least one root of characteristic polynomial expressible as

$$\begin{aligned}&\lambda^3 - \frac{L_3}{L_1L_3+M_1^2}\left(3\cdot\alpha\cdot i_C^2+\beta\right)\lambda^2\\ &+\frac{1}{L_3C}\left(1-\frac{M_1^2}{L_1L_3+M_1^2}\right)\lambda\\ &-\frac{1}{C\left(L_1L_3+M_1^2\right)}\left(1+3\cdot\alpha\cdot i_C^2\right)=0,\end{aligned} \tag{12}$$

and associated with fixed point at origin (where $i_C = 0$ A) need to have positive real part. For the existence of strange attractor, divergence of vector field calculated along orbit needs to be negative, at least on average. Divergence of vector field of dynamical system (9) is function of current i_C

$$\nabla\cdot\boldsymbol{F} = f\,(i_B) = \frac{L_3}{L_1L_3+M_1^2}\left(3\cdot\alpha\cdot i_C^2+\beta\right) < 0. \tag{13}$$

The last step is calculation of accurate flow quantifier that can be rapidly calculated, such as the largest Lyapunov exponent (LE) or, more general measure, dimension of state attractor. Since nature inspired optimization procedures are based on evaluation of population (group of solutions) and individual calculations of fitness functions are not mutually connected) it is also well-suited candidate for acceleration using multi-core computers and parallelization of processes. This can make convergence in lower dimensional parameter space rather fast.

This is the right place to point out that fixing unity values of accumulation elements $L_1 = L_3 = 1$ H and $C = 1$ F does not violate requirements mentioned above. Since parameter α associated with cubic term of polynomial trans-resistance plays attractor rescaling function rather than role of bifurcation parameter, only two parameters remain to be changed: magnetic coupling M_1 and linear term of trans-resistance β.

From the circuit theory point of view, magnetic coupling coefficient is a real number between zero and unity. Under this final restriction $M_1 \in (0, 1)$ and for negative α, vector field is dissipative in each point (regardless of i_C) and discovered set of parameters leading to robust chaotic solution is

$$M_1 = 680\,mH, \quad \alpha = -1V^3A^{-1}, \ \beta = 1.05\Omega. \tag{14}$$

This is indeed a physically reasonable combination of circuit parameters; normalized with respect to time and impedance. The numerical value of M_1 represents tight coupling, but still a practically implementable magnetic coupling coefficient. For parameter set (14), local vector field geometry around origin is composed by stable eigenplane and eigenvector, i.e., eigenvalues are

$$\lambda_{1,2} = -0.078 \pm j0.903, \quad \lambda_3 = 0.875. \tag{15}$$

Simultaneously, both fixed points located at exterior of vector field are full repellors with strong spiral movement. Geometry of vector field in the close neighborhood of these equilibrium point is characterized by following set of eigenvalues

$$\lambda_{1,2} = 0.33 \pm j0.733, \quad \lambda_3 = 0.057. \tag{16}$$

A typical strange attractor evolved for a group of parameters (14) together with initial conditions $\mathbf{x}_0$ =(100 mV, 0 A, 0 A)^T is graphically visualized in Fig. 5. For this numerical integration, the fourth order Runge-Kutta method with fixed step size (set to 10 ms) was adopted, and final time 2000 s. Figure 5 shows that solution of dynamical system (9) together with parameters (14) is highly sensitive to small changes of initial conditions. To prove this, a group of 10^4 initial conditions was generated around the origin of state space, adopting uniform distribution, and forming a cube with edge 0.01 (black points). Then, final states are stored after 1 s (red points), 10 s (green points) and 100 s (blue dots) long time evolution. Starting with initial conditions spread near state space origin, the most expanding direction is along i_C axis. Poincare sections reduce 3D problem into 2D map; slices are provided for zero voltage across capacitor and zero current through inductor in series. The geometric shape of observed typical strange attractor resembles popular double-scroll attractor; spirals are evolved around unstable fixed points placed in exterior positions (11). Before merged together, two single-scroll attractors exist and can be captured also via careful experimental measurement. Recurrence plots [25], time-vs-time visualization where signal periodicity and self-similarity of its time domain segments can be

judged. For this numerical analysis, the following group of parameters was used: final time 500 s, time step 10 ms and radius of sphere 0.05. If trajectory (only two coordinates are visualized) returns within this small state space distance it leads to successive detection of orbit repeating. For parameter set (14) with slightly increased value of cubic polynomial term $\alpha = -4$ V^3A^{-1} strange attractor shrinks and occupies relatively small fragment of state space. By considering dimensionless mathematical model, maximal value among all state variables does not exceed 1.2 (for default α maximal value is about 2.2). Attractor compression feature can be useful from viewpoint of full on-chip realization of chaotic oscillator. Especially for low power dissipation applications, where supply voltage is low as well, robust and small-sized strange attractors are welcomed. More details about this topic can be found in papers [26], [27]. Of course, too large amplitudes of generated signals are not the only concern of fully integrated analog chaotic oscillators. Process-voltage-temperature variations can cause serious problems as well, as demonstrated in tutorial papers [28], [29]. There, authors nicely explained what needs to be done to construct operational transconductance amplifier (OTA) based lumped chaotic systems resistant to common fabrication process-oriented problems. As was done in case of this paper, metaheuristics is used to find optimal values of chaotic system internal parameters. The proposed approach is validated via layout and post-layout simulations. Circuitry realization of dynamical system should always be preceded by sufficiently deep numerical analysis. Systematic design process toward OTA based chaotic oscillator and its CMOS realization is described in paper [30]. Authors adopt well known Lorenz system and show how Matlab/Simulink software can be used to implement both mathematical model of this system and its application in master-slave synchronization. Besides these results, authors showed method how chaotic state attractor can be rescaled, i.e., how to decrease amplitudes of generated waveforms without qualitative change of global dynamics. For 180 nm UMC integrated circuit technology, rescaling was performed via first and second order filters with predefined transfer function using Laplace transforms.

Fragments of parameter space where chaos can be localized are visualized by means of Fig. 6. The largest LE is 0.166 and corresponding Kaplan-Yorke dimension is close to value 2.28. High value of the largest LE occurs at upper boundaries of M_1 and β, one step before state trajectory becomes unbounded. Degree of disorderliness of time-domain sequences associated with generated signals can be judged via approximate entropy (AE) concept. In our case, the maximal value of AE [31], [32] derived from 500 s long time sequence that represents voltage across capacitor is 0.334. Note that combination of parameters M_1 and β that leads to the largest positive LE does not directly corresponds to combination for the highest value of AE. Simultaneously, places where state space attractor possesses the greatest value of metric dimension are also different if compared to maximal AE.

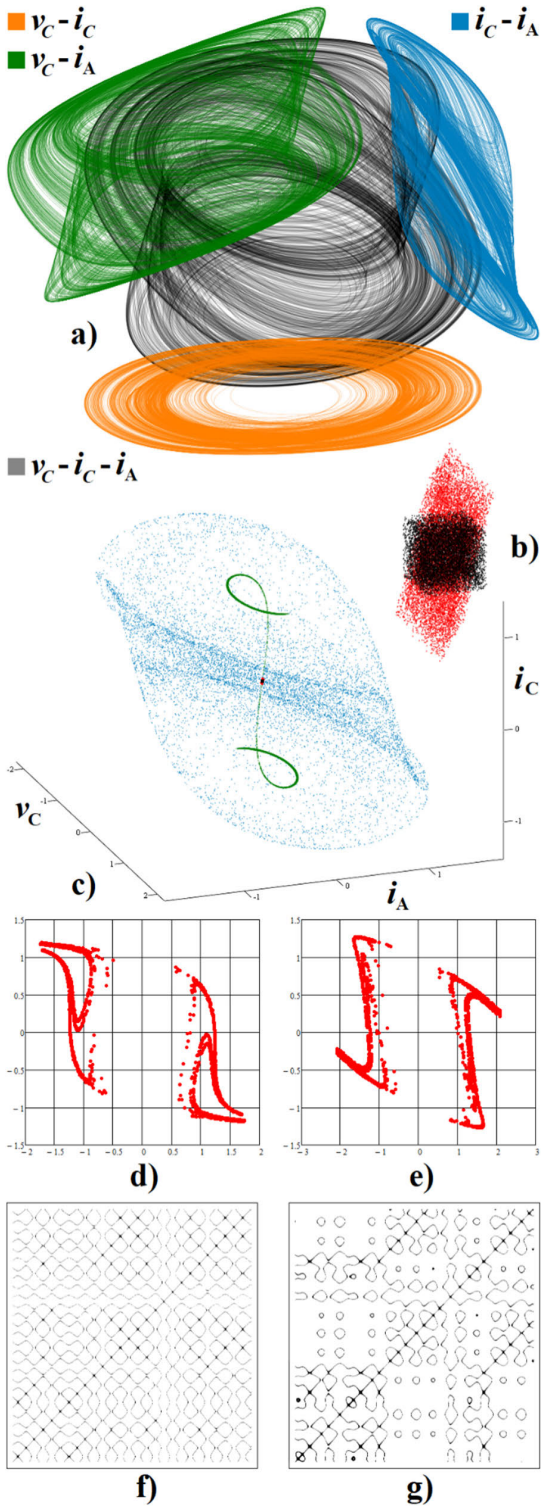

FIGURE 5. Few selected numerical results: a) phase portraits of typical strange attractor generated by system (9) having parameter group (14), b) group of 10^4 initial conditions with zoom on short time trajectory separation process, c) sensitivity demonstration, d) e) $v_C = 0$ V and $i_A = 0$ A cross-sections of typical attractor, f) g) recurrence plots calculated for state variable $v_C(t)$ and $i_B(t)$ respectively.

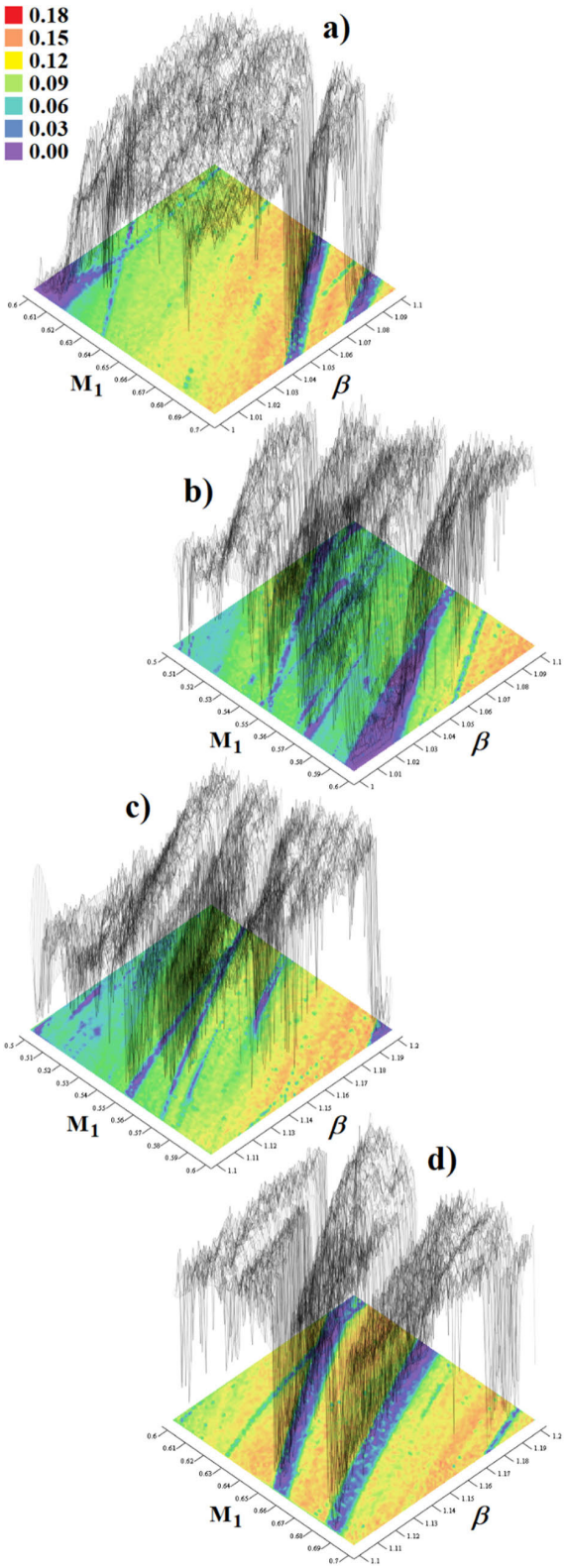

FIGURE 6. Rainbow-scaled surface-contour plots of the largest LE as 2D function of key system parameters: a) $M_1 \in (0.6, 0.7)$ H, $\beta \in (1, 1.1)$ Ω, b) $M_1 \in (0.5, 0.6)$ H, $\beta \in (1, 1.1)$ Ω, c) $M_1 \in (0.5, 0.6)$ H, $\beta \in (1.1, 1.2)$ Ω, and d) $M_1 \in (0.6, 0.7)$ H, $\beta \in (1.1, 1.2)$ Ω. Each plot contains 101 × 101 points.

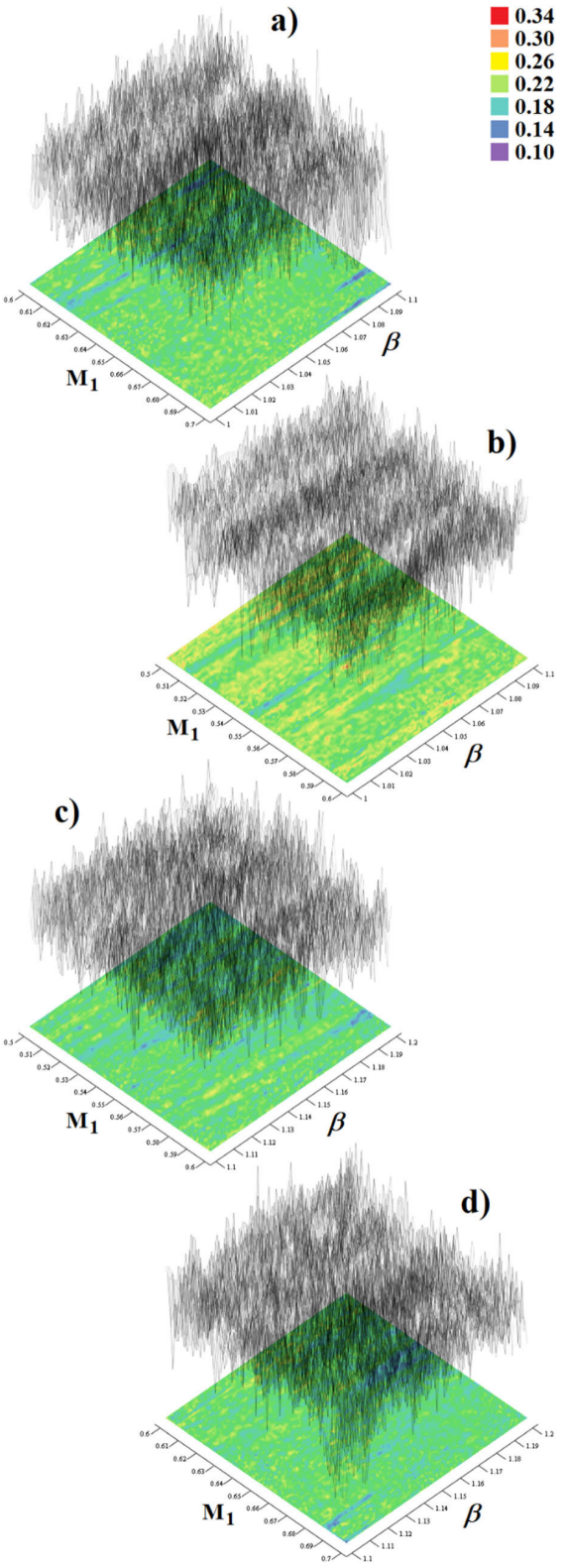

FIGURE 7. Rainbow-scaled surface-contour plots of AE as 2D function of key internal system parameters: a) $M_1 \in (0.6, 0.7)$ H, $\beta \in (1, 1.1)$ Ω, b) $M_1 \in (0.5, 0.6)$ H, $\beta \in (1, 1.1)$ Ω, c) $M_1 \in (0.5, 0.6)$ H, $\beta \in (1.1, 1.2)$ Ω, and d) $M_1 \in (0.6, 0.7)$ H, $\beta \in (1.1, 1.2)$ Ω. Each plot contains 101 × 101 points.

Figure 7 shows rainbow-scaled two-dimensional plot of AE as function of system key parameters. Note that the graphical pattern suggesting chaotic behavior is different if compared to profile of the largest LE. Graphical visualization

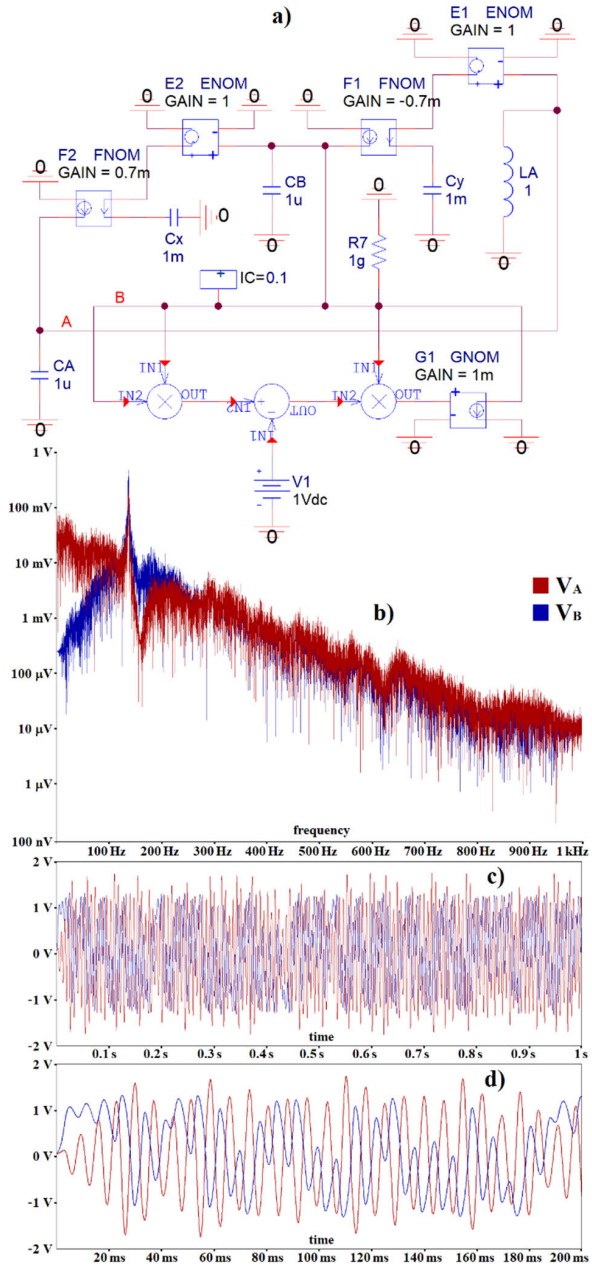

FIGURE 8. Orcad Pspice simulation of chaotic system dual to Reinartz chaotic oscillator: a) implementation using the ideal controlled sources, b) frequency spectra of voltages across working grounded capacitors, time-domain waveforms: c) long-time evolution, and d) zoomed pattern.

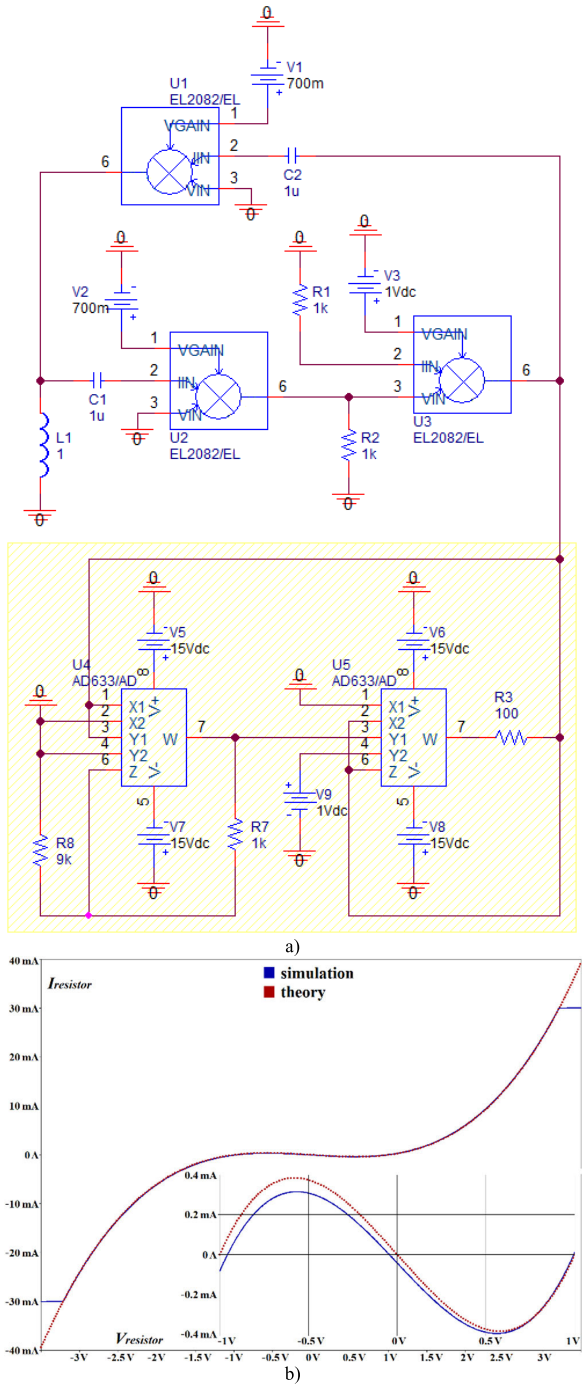

FIGURE 9. Dual Reinartz oscillator: a) circuitry realization using off-the-shelf components, b) Orcad Pspice simulation of ampere-voltage curve of polynomial resistor, calculated in interval of input voltages −3.5 V to 3.5 V and zoomed area from −1 V up to 1V, both with voltage step 1 mV.

of AE results shows that generated waveform exhibits significant level of entropic properties for many combinations of magnetic coupling and linear term of forward transresistance.

IV. EXPERIMENTAL VERIFICATION

True experimental verification via analog circuit construction and measurement belongs to standard and logical step when presenting new chaotic dynamical system [33]. Also, it clearly represents a step that can hardly be taken over by artificial intelligence [34].

Numerical analysis as well as circuit simulations are based on problem discretization, it means that solution is available at discrete instances of time, is burdened by rounding errors and errors caused by finite precision of chosen integration method. On the other hand, real practical measurement offers smooth integration and, if circuit time constants are reasonably short, transient behavior is visually uncapturable.

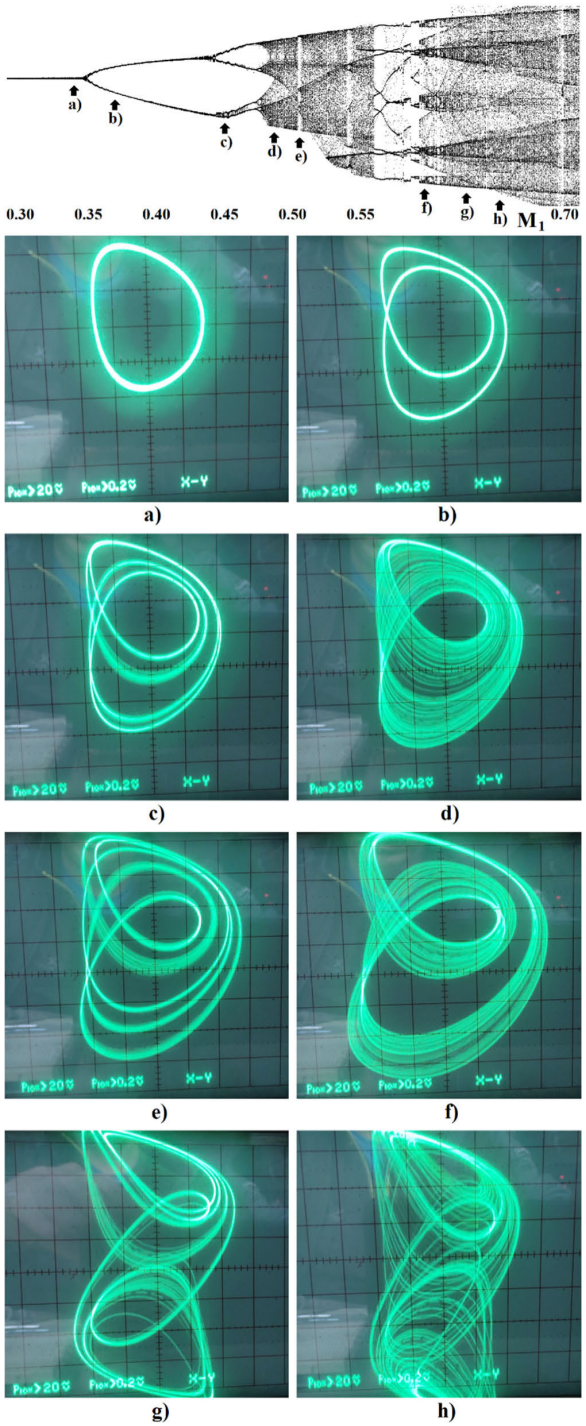

FIGURE 10. 1D bifurcation diagram calculated for magnetic coupling in interval $M_1 \in (0.2, 0.6)$ H with step 500 μH and experimentally confirmed route-to-chaos scenario via period-doubling sequence.

FPGA based implementations of autonomous dynamical systems can be found in many research papers, tutorials and studies. For example, authors in work [35] illustrate FPGA implementation of mechanical jerk function by synthesizing the discrete equations which are the result of one-step numerical integration method. After successful construction, obtained oscilloscope screenshots are compared with Matlab simulation outputs. Paper [36] demonstrate that only three building blocks are necessary to practically realize FPGA based 3D jerk systems, namely multipliers, adders and subtractors. Interesting feature of investigated systems is the presence of stable equilibrium, i.e., dynamics that exhibits hidden chaotic attractors. Authors conclude very good agreement between experimental observations and numerical integration results. New chaotic dynamical system and, after discretization of ordinary differential equations, FPGA based implementation of this system is one of topics of paper [37]. Authors propose pseudo-random number generator with this FPGA part followed by successful NIST randomness analysis. Of course, other interesting papers can be cited here, proving that FPGA based implementation of dynamical systems forms a bridge between numerical analysis and analog realization.

The most straightforward circuit synthesis method toward chaotic oscillator is based on integrator block schematic of mathematical model. A very nice comprehensive review paper thoroughly clarifying this synthesis method is [38]. Besides this, there are many papers [39], [40], [41], [42] where curious readers can find case studies, design examples, both simple and complex. A common disadvantage of these designs is the necessity to use many active and passive circuit elements. Moreover, one parameter associated with the initial mathematical model is often represented by several parameters of final circuit. Therefore, to observe 1D bifurcation scenario, simultaneous change of several circuit parameters is needed. For example, change of M_1 within presumptive analog computer-based realization of system (9) will be quite problematic. Fortunately, there are other ways nonlinear dynamical systems can be realized.

Since continuous smooth change of transformer´s magnetic coupling as well as achieving its accurate specific value up to decimal place is impossible in practice, linear transformer could be substituted by its dual, synthetic analog equivalent. Principal schematic is depicted in Fig. 8, where the form of static coupling is considered. Due to reciprocity, following equalities $C_x = C_y$ and $E_1 \cdot F_1 = \pm E_2 \cdot F_2$ need to be respected, i.e., "electrostatic transformer" is lossless. Behavior of developed circuit is uniquely determined by set of following ODE

$$\begin{aligned}
\frac{d}{dt} i_A &= -\frac{1}{L_A} v_A \\
\frac{d}{dt} v_A &= \frac{1}{C_A}\left[i_A + E_2 \cdot F_2 \cdot C_X \frac{d}{dt} v_B \right] \\
\frac{d}{dt} v_B &= \frac{1}{C_B}\left[-E_1 \cdot F_1 \cdot C_Y \frac{d}{dt} v_A + G_1 \cdot V_1 \cdot v_B - G_1 \cdot v_B^3 \right],
\end{aligned} \tag{17}$$

where electrostatic coupling coefficients $E_{1,2}$ are in Coulombs. Numerical values provided in schematic adopt impedance and frequency scaling factors, both equal to 10^3. Nonlinear resistor is implemented by one ideal differentiation block (DIFF), two multiplication blocks (MULT) and output

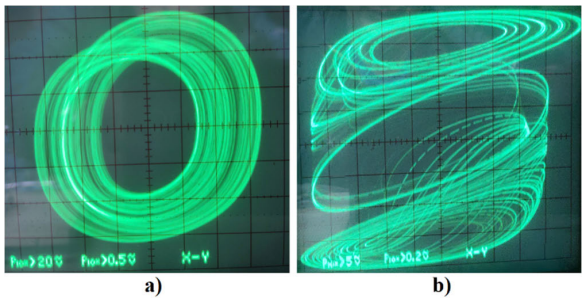

FIGURE 11. Plane projections of typical strange attractor generated by chaotic third-order system derived from reduced Reinartz sinusoidal oscillator: a) v_C vs i_C, b) i_C vs i_B.

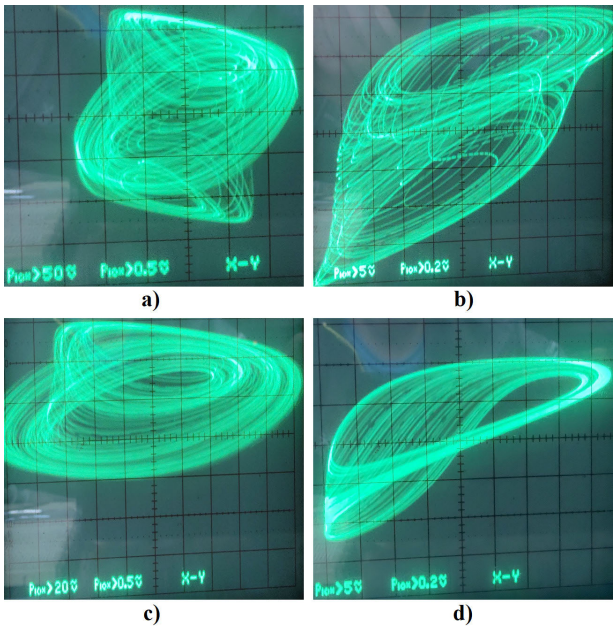

FIGURE 12. Selected plane projections of interestingly shaped chaotic attractors captured during experimental investigation of third order Reinartz-like oscillator.

voltage controlled current source G. Parameter β can be changed by voltage V_1. Resistor R_7 is redundant and creates non-zero admittance from node to ground as required by simulator. Pseudo-component IC1 serves to impose non-zero initial conditions.

Next step is to replace ideal blocks by real commercially available integrated circuits. The nonlinear part of vector field can be realized by a cascade of two four-quadrant analog multipliers AD633, see yellow area in Fig. 9. This figure also shows the difference between simulated and theoretical shape of ampere-voltage characteristic of nonlinear resistor. Within working range of input voltage (about ± 1.5 V for typical chaotic attractor) nonlinear resistor distributes less than 2 mA. Each pair of properly coupled ideal controlled sources, namely current-controlled current source (F_k) and voltage-controlled voltage source (E_k), can be substituted by second-generation current conveyor [43]. To minimize the required number of these active devices, a negative variant was chosen, marked as EL2082. This versatile building block offers the possibility to control transfer value of conveyed current via external DC voltage source in the range from 0 V to 2 V. This property will be used to smoothly adjust numerical value of electrostatic coupling coefficient. If necessary, large value of inductor can be decreased by additional frequency scaling or, more likely, inductor is implemented as active grounded synthetic element. Dynamical behavior of circuit provided in Fig. 9 is determined by following set of ordinary differential equations

$$\begin{aligned}
\frac{d}{dt} i_{L1} &= -\frac{1}{L_1} v_1 \\
\frac{d}{dt} v_1 &= \frac{1}{C_1}\left[i_{L1} + V_1 \cdot C_2 \frac{d}{dt} v_3 \right] \\
\frac{d}{dt} v_3 &= \frac{1}{C_2}\left[-V_2 \cdot V_3 \cdot \frac{R_2}{R_1} \cdot C_1 \frac{d}{dt} v_1 + \frac{V_9 \cdot v_3 - v_3^3}{R_3} \right],
\end{aligned} \tag{18}$$

where v_1 and v_3 are voltages measured at current outputs of integrated circuits U1 and U3 respectively. Resistors R_7 and R_8 do not take part in differential equations since these serve for compensation of internal transfer constant 0.1 of first analog multiplier (integrated circuit marked as U4).

Experimental verification of the chaotic nature of reduced Reinartz oscillator is represented by oscilloscope screenshots, see X-Y displays in Fig. 10, Fig. 11, and Fig. 12.

V. CONCLUSION

This brief paper demonstrates that significantly simplified configuration of the Reinartz oscillator can produce robust chaotic waveforms. The suggested simplification is based on specific working regime of generalized bipolar transistor and missing (negligible) magnetic coupling between two coils. Via numerical and experimental tests, it has been proved that generated strange attractors are neither numerical artifact nor long transient behavior. Searching for chaos routine went through element-reducing of circuit model used in practice. It results in a final dynamical system having two parameters; and each can be used to trace unique route-to-chaos scenario. Since one bifurcation parameter is remaining one magnetic coupling, which is very hard to adjust precisely, alternative synthesis of nonlinear dynamical system is applied. Selected oscilloscope screenshots are provided to clearly show that desired strange attractors are structurally stable.

The importance of study presented in this paper is not only in finding new chaotic dynamical system. Structural stability of observed strange attractor and its distinct unpredictability (promising positive value of the largest LE) predetermine it for practical signal processing applications. The component count of the new chaotic oscillator is the least possible: linear transformer, capacitor, and nonlinear resistor. Such amount of circuit elements is comparable to canonical chaotic circuits with memristor [44]. Simultaneously, real circuit realization of discovered chaotic system can be simple; even simpler than specific network designed, described, and experimentally

verified in this paper. Having magnetic coupling coefficient of real transformer measured, mathematical model of proposed third-order dynamical system can be rescaled accordingly to this numerical value. Then, the final chaotic oscillator can be constructed by following the original three component circuit configuration.

REFERENCES

[1] K. S. Halle, C. W. Wu, M. Itoh, and L. O. Chua, "Spread spectrum communication through modulation of chaos," *Int. J. Bifurcation Chaos*, vol. 3, no. 2, pp. 469–477, Apr. 1993, doi: 10.1142/s0218127493000374.

[2] C. Bai, H.-P. Ren, W.-Y. Zheng, and C. Grebogi, "Radio-wave communication with chaos," *IEEE Access*, vol. 8, pp. 167019–167026, 2020, doi: 10.1109/ACCESS.2020.3022632.

[3] M. Miao, L. Wang, M. Katz, and W. Xu, "Hybrid modulation scheme combining PPM with differential chaos shift keying modulation," *IEEE Wireless Commun. Lett.*, vol. 8, no. 2, pp. 340–343, Apr. 2019, doi: 10.1109/LWC.2018.2871137.

[4] J. Hwang, G. Kale, P. P. Patel, R. Vishwakarma, M. Aliasgari, A. Hedayatipour, A. Rezaei, and H. Sayadi, "Machine learning in chaos-based encryption: Theory, implementations, and applications," *IEEE Access*, vol. 11, pp. 125749–125767, 2023, doi: 10.1109/ACCESS.2023.3331320.

[5] J. S. Teh, M. Alawida, and Y. C. Sii, "Implementation and practical problems of chaos-based cryptography revisited," *J. Inf. Secur. Appl.*, vol. 50, Feb. 2020, Art. no. 102421, doi: 10.1016/j.jisa.2019.102421.

[6] S. Mobayen, C. Volos, Ü. Çavuşoğlu, and S. S. Kaçar, "A simple chaotic flow with hyperbolic sinusoidal function and its application to voice encryption," *Symmetry*, vol. 12, no. 12, p. 2047, Dec. 2020, doi: 10.3390/sym12122047.

[7] S. Bowong, F. M. M. Kakmeni, and R. Koina, "A new synchronization principle for a class of Lur'e systems with applications in secure communication," *Int. J. Bifurcation Chaos*, vol. 14, no. 7, pp. 2477–2491, Jul. 2004, doi: 10.1142/s0218127404010758.

[8] M. Shafiq, I. Ahmad, and B. Naderi, "Synchronization of chaotic RCL shunted-Josephson junction systems with unknown parametric uncertainties: Applications to secure communication systems," *IEEE Access*, vol. 11, pp. 68943–68960, 2023, doi: 10.1109/ACCESS.2023.3286015.

[9] M. Drutarovsky and P. Galajda, "A robust chaos-based true random number generator embedded in reconfigurable switched-capacitor hardware," *Radioengineering*, vol. 16, no. 3, pp. 120–127, 2007.

[10] J. C. Sprott and W. J. Thio, "A chaotic circuit for producing Gaussian random numbers," *Int. J. Bifurcation Chaos*, vol. 30, no. 8, Jun. 2020, Art. no. 2050116, doi: 10.1142/s0218127420501163.

[11] J. Petrzela, "Chaos in analog electronic circuits: Comprehensive review, solved problems, open topics and small example," *Mathematics*, vol. 10, no. 21, p. 4108, Nov. 2022, doi: 10.3390/math10214108.

[12] R. Kiliç and F. Yildirim, "A survey of Wien bridge-based chaotic oscillators: Design and experimental issues," *Chaos, Solitons Fractals*, vol. 38, no. 5, pp. 1394–1410, Dec. 2008, doi: 10.1016/j.chaos.2008.02.016.

[13] K. Rajagopal, C. Li, F. Nazarimehr, A. Karthikeyan, P. Duraisamy, and S. Jafari, "Chaotic dynamics of modified Wien bridge oscillator with fractional order memristor," *Radioengineering*, vol. 27, no. 1, pp. 165–174, Apr. 2019, doi: 10.13164/re.2019.0165.

[14] Y. Hosokawa, Y. Nishio, and A. Ushida, "Analysis of chaotic phenomena in two RC phase shift oscillators coupled by a diode," *IEICE Trans. Fundam.*, vol. E84, no. 9, pp. 2288–2295, 2001.

[15] M. P. Kennedy, "Chaos in the colpitts oscillator," *IEEE Trans. Circuits Syst. I, Fundam. Theory Appl.*, vol. 41, no. 11, pp. 771–774, Nov. 1994, doi: 10.1109/81.331536.

[16] R. B. W. Tekam, J. Kengne, and G. D. Kenmoe, "High frequency Colpitts' oscillator: A simple configuration for chaos generation," *Chaos, Solitons Fractals*, vol. 126, pp. 351–360, Sep. 2019, doi: 10.1016/j.chaos.2019.07.020.

[17] J. Kengne, J. C. Chedjou, V. A. Fono, and K. Kyamakya, "On the analysis of bipolar transistor based chaotic circuits: Case of a two-stage colpitts oscillator," *Nonlinear Dyn.*, vol. 67, no. 2, pp. 1247–1260, Jan. 2012, doi: 10.1007/s11071-011-0066-7.

[18] K. Peter, "Chaos in Hartley's oscillator," *Int. J. Bifurcation Chaos*, vol. 12, no. 10, pp. 2229–2232, Oct. 2002, doi: 10.1142/s0218127402005777.

[19] R. Tchitnga, H. B. Fotsin, B. Nana, P. H. L. Fotso, and P. Woafo, "Hartley's oscillator: The simplest chaotic two-component circuit," *Chaos, Solitons Fractals*, vol. 45, no. 3, pp. 306–313, Mar. 2012, doi: 10.1016/j.chaos.2011.12.017.

[20] J. Petrzela, "Chaotic and hyperchaotic dynamics of a clapp oscillator," *Mathematics*, vol. 10, no. 11, p. 1868, May 2022, doi: 10.3390/math10111868.

[21] J. Petrzela, "Chaotic states of transistor-based tuned-collector oscillator," *Mathematics*, vol. 11, no. 9, p. 2213, May 2023, doi: 10.3390/math11092213.

[22] L. Keuninckx, G. Van der Sande, and J. Danckaert, "Simple two-transistor single-supply resistor–capacitor chaotic oscillator," *IEEE Trans. Circuits Syst. II, Exp. Briefs*, vol. 62, no. 9, pp. 891–895, Sep. 2015, doi: 10.1109/TCSII.2015.2435211.

[23] L. Minati, M. Frasca, P. Oświęcimka, L. Faes, and S. Drożdż, "Atypical transistor-based chaotic oscillators: Design, realization, and diversity," *Chaos, Interdiscipl. J. Nonlinear Sci.*, vol. 27, no. 7, Jul. 2017, Art. no. 073113, doi: 10.1063/1.4994815.

[24] J. Petrzela, "Chaotic steady states of the reinartz oscillator: Mathematical evidence and experimental confirmation," *Axioms*, vol. 12, no. 12, p. 1101, Dec. 2023, doi: 10.3390/axioms12121101.

[25] Y. Zhou, S. Gao, M. Sun, Y. Zhou, Z. Chen, and J. Zhang, "Recognizing chaos by deep learning and transfer learning on recurrence plots," *Int. J. Bifurcation Chaos*, vol. 33, no. 10, Aug. 2023, Art. no. 2350116, doi: 10.1142/s021812742350116x.

[26] M. A. Valencia-Ponce, A. M. González-Zapata, L. G. de la Fraga, C. Sanchez-Lopez, and E. Tlelo-Cuautle, "Integrated circuit design of fractional-order chaotic systems optimized by metaheuristics," *Electronics*, vol. 12, no. 2, p. 413, Jan. 2023, doi: 10.3390/electronics12020413.

[27] R. Trejo-Guerra, E. Tlelo-Cuautle, V. H. Carbajal-Gómez, and G. Rodriguez-Gómez, "A survey on the integrated design of chaotic oscillators," *Appl. Math. Comput.*, vol. 219, no. 10, pp. 5113–5122, Jan. 2013, doi: 10.1016/j.amc.2012.11.021.

[28] V. Carbajal-Gomez, E. Tlelo-Cuautle, C. Sanchez-Lopez, and F. Fernandez-Fernandez, "PVT-robust CMOS programmable chaotic oscillator: Synchronization of two 7-scroll attractors," *Electronics*, vol. 7, no. 10, p. 252, Oct. 2018, doi: 10.3390/electronics7100252.

[29] V. H. Carbajal-Gomez, E. Tlelo-Cuautle, J. M. Munoz-Pacheco, L. G. de la Fraga, C. Sanchez-Lopez, and F. V. Fernandez-Fernandez, "Optimization and CMOS design of chaotic oscillators robust to PVT variations," *Integration*, vol. 65, no. 3, pp. 32–42, 2019, doi: 10.1016/j.vlsi.2018.10.010.

[30] E. Juarez-Mendoza, F. A. del Angel-Diaz, A. Diaz-Sanchez, and E. Tlelo-Cuautle, "CMOS design of chaotic systems using biquadratic OTA-C filters," *J. Low Power Electron. Appl.*, vol. 14, no. 1, p. 14, 2024, doi: 10.3390/jlpea14010014.

[31] S. M. Pincus, "Approximate entropy as a measure of system complexity," *Proc. Nat. Acad. Sci. USA*, vol. 88, no. 6, pp. 2297–2301, Mar. 1991, doi: 10.1073/pnas.88.6.2297.

[32] A. Delgado-Bonal and A. Marshak, "Approximate entropy and sample entropy: A comprehensive tutorial," *Entropy*, vol. 21, no. 6, p. 541, May 2019, doi: 10.3390/e21060541.

[33] J. C. Sprott, "A proposed standard for the publication of new chaotic systems," *Int. J. Bifurcation Chaos*, vol. 21, no. 9, pp. 2391–2394, Sep. 2011, doi: 10.1142/s021812741103009x.

[34] J. C. Sprott, "Artificial intelligence study of the system JCS-08-13-2022," *Int. J. Bifurcation Chaos*, vol. 32, no. 12, Sep. 2022, Art. no. 2230028, doi: 10.1142/s0218127422300282.

[35] S. Vaidyanathan, E. Tlelo-Cuautle, K. Benkouider, A. Sambas, and B. Ovilla-Martinez, "FPGA-based implementation of a new 3-D multistable chaotic jerk system with two unstable balance points," *Technologies*, vol. 11, no. 4, p. 92, 2023, doi: 10.3390/technologies11040092.

[36] S. Vaidyanathan, A. T. Azar, I. A. Hameed, K. Benkouider, E. Tlelo-Cuautle, B. Ovilla-Martinez, C.-H. Lien, and A. Sambas, "Bifurcation analysis, synchronization and FPGA implementation of a new 3-D jerk system with a stable equilibrium," *Mathematics*, vol. 11, no. 12, p. 2623, Jun. 2023, doi: 10.3390/math11122623.

[37] A. Sambas, S. Vaidyanathan, X. Zhang, I. Koyuncu, T. Bonny, M. Tuna, M. Alçin, S. Zhang, I. Mohammed Sulaiman, A. M. Awwal, and P. Kumam, "A novel 3D chaotic system with line equilibrium: Multistability, integral sliding mode control, electronic circuit, FPGA implementation and its image encryption," *IEEE Access*, vol. 10, pp. 68057–68074, 2022, doi: 10.1109/ACCESS.2022.3181424.

[38] M. Itoh, "Synthesis of electronic circuits for simulating nonlinear dynamics," *Int. J. Bifurcation Chaos*, vol. 11, no. 3, pp. 605–653, Mar. 2001, doi: 10.1142/s0218127401002341.
[39] V. T. Pham, D. S. Ali, N. M. G. Al-Saidi, K. Rajagopal, F. E. Alsaadi, and S. Jafari, "A novel mega-stable chaotic circuit," *Radioengineering*, vol. 29, no. 1, pp. 140–146, Apr. 2020, doi: 10.13164/re.2020.0140.
[40] J. Petrzela and T. Gotthans, "New chaotic dynamical system with a conic-shaped equilibrium located on the plane structure," *Appl. Sci.*, vol. 7, no. 10, p. 976, 2017, doi: 10.3390/app7100976.
[41] C. Nwachioma, J. Humberto Pérez-Cruz, A. Jiménez, M. Ezuma, and R. Rivera-Blas, "A new chaotic oscillator—Properties, analog implementation, and secure communication application," *IEEE Access*, vol. 7, pp. 7510–7521, 2019, doi: 10.1109/ACCESS.2018.2889964.
[42] R. Lu, H. Natiq, A. M. A. Ali, and Y. Zhu, "Synchronization of dissipative Nosé–Hoover systems: Circuit implementation," *Radioengineering*, vol. 32, no. 4, pp. 511–522, Dec. 2023, doi: 10.13164/re.2023.0511.
[43] J. Petrzela, "Strange attractors generated by multiple-valued static memory cell with polynomial approximation of resonant tunneling diodes," *Entropy*, vol. 20, no. 9, p. 697, Sep. 2018, doi: 10.3390/e20090697.
[44] B. Muthuswamy and L. O. Chua, "Simplest chaotic circuit," *Int. J. Bifurcation Chaos*, vol. 20, no. 5, pp. 1567–1580, May 2010, doi: 10.1142/s0218127410027076.

JIRI PETRZELA was born in Brno, Czech Republic, in 1978. He received the M.Sc. and Ph.D. degrees in theoretical electronics from Brno University of Technology, in 2003 and 2007, respectively. He is currently an Associate Professor with the Department of Electrical Engineering, Faculty of Military Technology, University of Defence, Brno. He is the main author or coauthor of more than 40 journal articles and 60 international conference contributions. His research interests include numerical methods in electrical engineering, nonlinear dynamics, chaos theory, and analog lumped circuit design.

ONDREJ KALLER was born in Frýdlant nad Ostravicí, Czech Republic, in 1986. He received the M.Sc. and Ph.D. degrees in radio electronics from Brno University of Technology, in 2010 and 2017, respectively. Currently, he is a Postdoctoral Academic and a Researcher with the Department of Electrical Engineering, Faculty of Military Technology, University of Defence, Brno, Czech Republic. His research interests include analog signal processing, computer-aided analysis of lumped circuits, modeling, and measurement of radio-frequency functional blocks.

JIRI VAVRA received the M.S. and Ph.D. degrees from the Faculty of Electrical Engineering and Communication, Brno University of Technology, Czech Republic, in 2007 and 2012, respectively. Currently, he is an Associate Professor with the Department of Electrical Engineering, University of Defence, Brno, Czech Republic. His research interests include analog signal processing, especially to current-mode circuits, frequency filters, and mem-systems.